Beyond perfusion: measuring water transport across brain barriers with arterial spin labeling MRI

Petitclerc, L.

Chapter 2

Combining T_2 Measurements and Crusher Gradients Into a Single ASL Sequence for Comparison of the Measurement of Water Transport Across the Blood-Brain Barrier

L. Petitclerc[1,2], S. Schmid[1,2], L. Hirschler[1], M.J.P. van Osch[1,2]

[1.] *Gorter Center for High Field MRI, Department of Radiology, Leiden University Medical Center, Leiden, Netherlands*
[2.] *Leiden Institute for Brain and Cognition, Leiden, Netherlands*

Published as full paper in: Magnetic Resonance in Medicine, 2021; 85(5):2649–2660.

2.0 ABSTRACT

Purpose: Arterial Spin Labeling can be used to assess the transition-time of water molecules across the blood-brain barrier (BBB), when combined with sequence modules which allow a separation of intravascular from tissue signal. The bipolar gradient technique measures the intravascular fraction by removing flowing spins. The T_2-relaxation-under-spin-tagging (TRUST) technique modulates the echo time to differentiate between intra- and extra-vascular spins based upon T_2. These modules were combined into a single time-encoded pCASL sequence to compare their mechanisms of action as well as their assessment of water transition across the BBB.

Methods: This protocol was acquired on a Philips Ingenia-CX scanner, with 9 healthy volunteers who provided written informed consent. The sequence consisted of a Hadamard-encoded pCASL labeling module, followed by the TRUST module (effective echo times of 0, 40 and 80 ms) and bipolar flow-crushing gradients (2, 4 and ∞ cm/s). An additional experiment was performed with TRUST and a 3D-GRASE readout.

Results: Gradients imperfectly cancelled the intravascular signal, as evidenced by the presence of residual signal in the arteries at early PLDs as well as the underestimation of the intravascular fraction as compared to the TRUST method. The TRUST module allowed to detect the transport of water deeper into the vascular tree through changes in T2 than the employed crusher gradients, with their limited b-value, could.

Conclusion: Of the implemented techniques, TRUST allowed to follow intravascular signal deeper into the vascular tree than the approach with (relatively weak) crusher gradients when quantifying the transport-time of water across the BBB.

Key words: Arterial Spin Labeling, TRUST, T2-prep, crusher gradients, bipolar gradients, blood-brain barrier

2.1 INTRODUCTION

The blood-brain barrier (BBB) is a boundary between the intravascular and extravascular spaces in the brain. Its role is to regulate the exchange of molecules such as nutrients between these spaces and prevent pathogens from entering. [1–3] Although many organs possess a similar membrane, the BBB distinguishes itself by the presence of very tight junctions which prohibit bulk flow of water. Water transport across the BBB is mediated in large part through aquaporin-4 channels[150] and is on the order of magnitude of diffusion.[1] By contrast, gadolinium-based contrast agent molecules cannot cross the healthy BBB because of their size. In pathology, the BBB progressively disintegrates and allows easier exchange of molecules, including contrast agents. BBB break down has been observed in neurodegenerative diseases such as Alzheimer's Disease [7,9] as well as in epilepsy, stroke, brain tumours and more generally in aging brains.[3,4] It remains unclear whether BBB disruptions are a cause or consequence of these neurological disorders.[4] Effective, non-invasive BBB characterization could shed light on this issue, by longitudinal monitoring of these disruptions.

There are several methods of assessing BBB integrity in vivo, each associated with their limitations. Nuclear medicine uses radio-labelled isotopes, which requires injection and exposure to ionizing radiation. The cerebrospinal fluid (CSF)/serum albumin ratio can show protein leakage into the CSF, but requires a lumbar puncture and gives no localized information. Contrast-enhanced computed tomography has similar issues as nuclear imaging.[13] In MRI, Gd-based contrast agents are used in dynamic susceptibility contrast imaging (DSC-MRI) as well as dynamic contrast-enhanced (DCE)-MRI, with the latter considered the gold standard in MRI-based BBB assessment. The need for contrast injection is a limiting factor for repeated measurements and it suffers from high variability between sites and protocols.[13] Moreover, in normally-functioning BBB, there is minimal transport of the Gd-based molecules to measure, limiting detection of early BBB-disruption. Water on the other hand is a much smaller molecule which is transported across the BBB at varying rates in health and disease, hence using it as a tracer could allow for the measurement of more subtle changes in BBB integrity.

Arterial Spin Labeling (ASL) is a method that measures tissue perfusion, using water as an endogenous tracer. Therefore, ASL contrast could be leveraged to measure the transport of water across the BBB in a non-invasive manner, provided the intravascular and extravascular water signal can be differentiated[151]. Two such methods are investigated in this study. The first is T_2-Relaxation-Under-Spin-Tagging (TRUST), which allows the localization of the label in the intravascular and extravascular compartments[142,143] by exploiting significant differences between blood and tissue T_2[144,145]. The second method applies bipolar crusher gradients (in literature both relatively weak crusher gradients that target fast flowing spins (b-values below

20 s/mm^2) as well as stronger, higher b-value gradients which target diffusing spins have been employed) which remove signal from the vasculature based upon the velocity of blood along the gradient direction, making it possible to calculate the proportion of signal in the vascular and tissue compartments.[111,131,132] Both methods have been used to investigate the distribution of the ASL signal in these compartments and its position along the vascular tree. Combining them with a dynamic method such as Hadamard-encoding[139,141] offers a time-resolved portrait of the transition across the BBB.[129,130,143,152] There has been no study directly comparing the results of TRUST and motion-sensitizing gradient techniques. This paper aims to accomplish this by combining both contrast mechanisms into a single time-encoded ASL sequence, as a means to gather more insight into their different mechanisms of action on the ASL signal and their comparative strengths and weaknesses in imaging the water transition across the BBB. In addition, after one of the methods appeared to be sensitive to the transition of the ASL signal deeper into the vasculature, it was combined on its own with a more efficient readout to reduce scan length to a more clinically relevant time frame, while improving signal quality.

2.2 METHODS

2.2.1 ASL Sequence

The main sequence in our protocol, shown schematically in figure 2.1, combined a Hadamard-8 pCASL preparation, followed by TRUST pulses before a 2D-EPI readout with bipolar gradients. The Hadamard-matrix block timings were chosen to encompass the full passage of the labelled water from large arteries to tissue perfusion. The first blocks are longer to compensate for the reduction in signal due to T1-relaxation, and the later blocks are shorter to provide a higher temporal resolution during the vascular phase. FOCI background suppression pulses were applied between blocks 2-3 and 6-7, a timing that was optimized to minimize signal from gray and white matter simultaneously. Within the dynamic imaging cycle (i.e. repeats of one complete Hadamard encoding-matrix), the different gradient and TRUST schemes were interleaved. Bipolar gradients were applied as crushers into the gradient echo readout, with three different velocity encodings (V_{enc}) of 2, 4, and ∞ (no gradient) cm/s, later referred to as the 100%, 50% and 0% strength gradients, respectively. When interpreting these as diffusion weighting gradients, b-values were 3.42, 0.85, and 0 s/mm^2, respectively. These gradients were applied in three perpendicular directions at once, resulting in a combined effective gradient of a factor √3 higher strength and effective b-values of 10.3, 2.57 and 0 s/mm^2 in the composite direction. TRUST consisted of a T_2-preparation module whose effect was to modify the effective echo time (eTE) of the sequence. The pulse train first incorporates a 90°-pulse, tipping magnetisation into the transverse plane, then followed by n equidistant 180° refocusing pulses to avoid T2* effects, and a final -90°-pulse to tip it

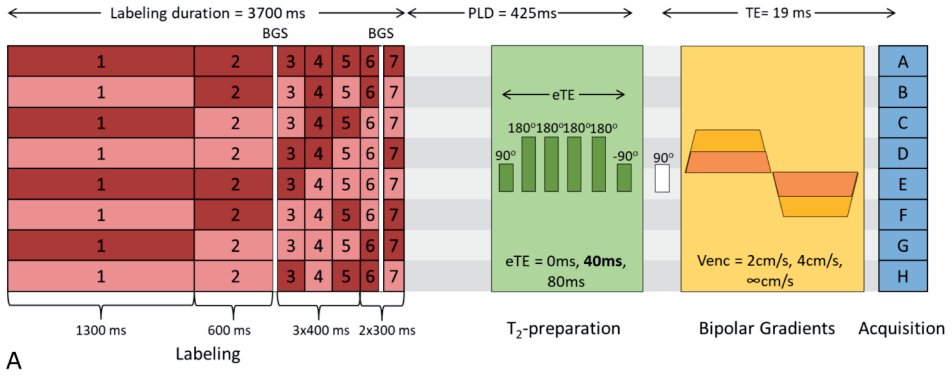

Dynamic #	Gradient Venc (cm/s)	eTE (ms)
1	∞	0
2		40
3		40
4		80
5		80
6		80
7-12	4	(repeat 1-6)
12-18	2	(repeat 1-6)

B

Figure 2.1. MRI sequence design. A) One of the lines of the Hadamard encoding matrix is applied (dark red: label, light red: control), followed by the TRUST T2 preparation module, then the bipolar gradient, and finally the image acquisition scheme. Labels A-H represent the 8 Hadamard images acquired following the corresponding line in the labeling scheme. B) The sequence interleaves the acquisition of different eTE's and gradient strengths within the dynamic cycle. BGS: background suppression pulse. PLD: post-labeling delay. eTE: effective echo-time. V_{enc}: encoding velocity.

back along the longitudinal axis. Three schemes were used: no module, with eTE = 0 ms; an n = 4 module, eTE = 40 ms; and an n = 8 module, eTE = 80 ms. More dynamics were acquired with longer eTEs to account for the lower SNR of these images. This resulted in an 18-dynamic scheme, illustrated in figure 2.1b, which was repeated four times. 11 slices of thickness 7 mm, without gap, were acquired, with an in-plane acquisition resolution of 3.2 × 3.2 mm^2, reconstructed at 2.75 × 2.75 mm^2 (field-of-view 220 × 220 mm^2, SENSE-factor 2.5, single shot EPI-readout, TE of 19 ms, TR of 4950 ms, total scan time of 50 minutes).

In total, 9 volunteers were examined with this protocol (6 male and 3 female, ages 21-36 years) and provided written informed consent in compliance with our institutional review board guidelines. All examinations were carried out on a 3T Ingenia-CX scanner (Philips, Best, The Netherlands) with a 32-channel head coil.

2.2.2 3D-GRASE Protocol

An additional scan was performed in one other subject (female, 43 years old), which focused on the use of a 3D readout in combination with the TRUST measurements. This approach adheres to the consensus recommendation of using a 3D readout with ASL[78], while showing the potential of the method for higher SNR in a shorter scan time when it is performed on its own without the combination with motion-sensitizing gradients. In this protocol, the same Hadamard preparation and BGS pulses were performed, followed by a T_2-prep module with eTE = 0, 40, 80 or 160 ms, and finally a 3D-GRASE readout (3 shots, two averages per eTE, 3.75 × 3.80 × 7 mm^3, SENSE 2.3 (RL), 11 slices while oversampling with a factor 1.8, reconstructed at 3 × 3 mm^2, TR/TE of 5100/10 ms, and scan time of 18min20s).

2.2.3 Data Analysis

All post-processing and analysis was performed in MATLAB (The Mathworks, Inc., Natick, MA). A schematic representation of the analysis pipeline is given in figure 2.2a. Hadamard-decoding was performed to extract the ASL signal at the seven post-labeling delays (PLDs). An arterial mask was created individually for each subject by thresholding the averaged ASL-image over the first three time points, and similarly in the gray matter using the average of images from the last two time points. The threshold was selected manually so that anatomical features were preserved (such as the circle of Willis in the arterial mask and the gyri of the gray matter) and a similar number of voxels were included for all subjects (1043 ± 165 for the arteries, 4488 ± 385 for the gray matter). Voxels contained in the arterial mask

were excluded from the gray matter mask. An example of this procedure is shown in figure 2.2b. All images were smoothed using a 2×2 voxel Gaussian kernel (σ = 1 voxel). The ASL signal was averaged over the arterial and gray matter masks separately and in combination. This resulted in signal curves through time for each combination of gradient strength and

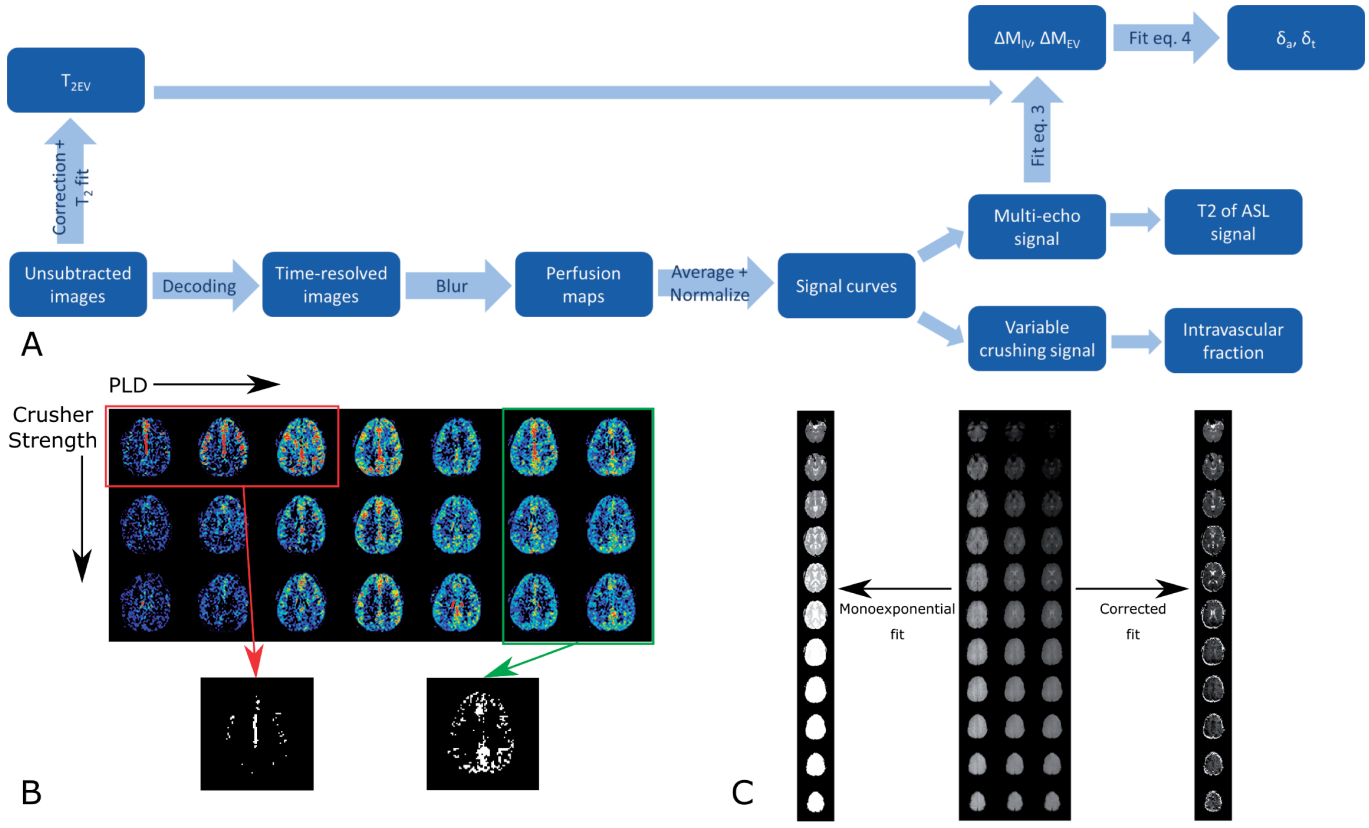

Figure 2.2. A) Data analysis pipeline. The masking step is shown in B: the three earliest time points of the uncrushed perfusion maps are averaged and thresholded to obtain the vascular mask. The two last time points of images from all crusher settings are averaged and thresholded for the gray matter mask, and any voxels from the arterial mask are removed. In C, the T_{2EV} maps without (left) and with correction (right) for the sequential slice acquisition are shown.

eTE. These values were normalized to the maximum of the non-crushed, eTE=0 ms curve for each subject.

The TRUST sequence allows the measurement of T_2, by fitting the monoexponential decay of the signal as a function of eTE. This calculation was conducted on the average signal of the whole sampled population in the gray matter and arteries, using the nlinfit MATLAB function. In the 3D sequence, the T_2 was calculated on a voxel-by-voxel basis after smoothing using a gaussian kernel (3×3 voxels, σ=2). The intravascular fraction of the signal was calculated using the crushed and non-crushed signal, assuming that the bipolar gradients would crush all signal inside the vasculature. The intravascular fraction was estimated as the percentage of the non-crushed signal that is removed by the application of gradients: IVF = 100×(non-crushed – crushed)/non-crushed.

2.2.4 Two-Compartment Dynamic Analysis

In order to quantitatively assess water transport across the BBB, a compartmental analysis was performed[150]. This is used to separate and fit the vascular and extravascular components of the signal, extracting timing parameters corresponding to the label arrival time in the vasculature (arterial transit time, δ_a) and in the tissue (tissue transit time, δ_t). The difference between these gives an estimate of the transport time across the BBB, or exchange time, T_{ex}.

First, the T_2 value of tissue (T_{2EV}) is calculated by fitting the multi-echo unsubtracted data to a monoexponential decay, which had to be modified to account for multi-slice acquisition (higher slices experience T_1 relaxation in the time between the T_2-prep module and the excitation pulse, leading to an apparent decrease in measured T_2):

$$S_c = S_0 \exp(-eTE/T_{2EV}) \quad \text{(Eq. 2.1)}$$

Where T_{2EV} is the tissue T_2 and S_c is the corrected unsubtracted signal:

$$S_c = \frac{(S_m - M_0(1-q))}{q}$$
$$q = exp\left(\frac{-((n-1)t_s + t_{2ex})}{T_{1GM}}\right) \quad \text{(Eq. 2.2)}$$

Where S_m is the measured signal, M_0 is the equilibrium magnetisation (measured in a separate scan), n is the slice number, from the inferior to the superior, t_s is the acquisition time per slice and t_{2ex} is the time between the application of the TRUST module and the first slice acquisition. The T_{2EV} maps obtained without and with this correction are shown in figure 2.2c, where the increase in T_2 from the bottom slice (top of the image) to the top in the

uncorrected images is clearly apparent. This step was omitted in the 3D dataset as the time between T2prep and readout does not vary across slices in that case.

The T_{2EV} calculated from the unsubtracted images was then included in the compartmental analysis:

$$\Delta M = \Delta M_{EV} exp(-eTE/T_{2EV}) + \Delta M_{IV} exp(-eTE/T_{2IV}) \quad \text{(Eq. 2.3)}$$

Where ΔM is the ASL signal, ΔM_{EV} and ΔM_{IV} are the parts of it that arise from the tissue and vascular compartments respectively, and T_{2EV} and T_{2IV} are the relaxation times for the corresponding compartments. All time points are fitted simultaneously, with $T2_{EV}$ taken from the unsubtracted signal and ΔM_{EV}, ΔM_{IV}, and $T2_{IV}$ fitted. Whereas the first two could vary, $T2_{IV}$ was held constant over the PLDs.

The dynamic model that was adapted from Ohene et al.[150], for pCASL instead of FAIR[153]:

$$\Delta M_{IV}(\omega,\tau) = \begin{cases} 0, \omega < \delta_a - \tau \\ 0, \omega \geq \delta_t \\ 2M_0 \frac{f}{\lambda} \alpha T_{1b} \left(\exp\left(\frac{(\min(\delta_a - \omega, 0) - \delta_a)}{T_{1b}} \right) - \exp\left(\frac{-\min(\omega + \tau, \delta_t)}{T_{1b}} \right) \right), otherwise \end{cases}$$

$$\Delta M_{EV}(\omega,\tau) = \begin{cases} 0, \omega + \tau < \delta_t \\ 2M_0 \frac{f}{\lambda} \alpha T_1' e^{-\delta_t / T_{1b}} \left(\exp\left(\frac{\min(\delta_a - \omega, 0)}{T_1'} \right) - \exp\left(\frac{(\delta_t - \omega - \tau)}{T_1'} \right) \right), otherwise \end{cases}$$

$$T_1' = \frac{1}{T_{1GM}} + \frac{f}{\lambda}$$

(Eq. 2.4)

Where ω is the PLD, τ is the length of the labeling block, f is CBF, λ is the blood-brain partition coefficient (λ = 0.9), α is the labeling efficiency (α = 0.85), and T_{1b} and T_{1GM} are the relaxation times of blood (T_{1b} = 1665 ms) and tissue (T_{1GM} = 1250 ms). This analysis was conducted separately on the data from the three crusher settings, in order to compare the effect of crusher strength on the calculated transit times. 95% confidence intervals on the fitted timing parameters were also reported. In the 3D dataset, this fit was performed on a voxel-by-voxel basis, resulting in parameter maps for T_2 at all time points, as well as δ_a, δ_t and T_{ex} in the gray matter.

2.3 RESULTS

2.3.1 ASL signal maps

Figure 2.3 shows the effect of variable gradient strengths on ASL signal maps for three slices in one subject. Early time points (PLD < 1025 ms) are characterized by the presence of high signal in the arteries, which is removed by bipolar gradients. Although the effect for the weaker gradient is already large, there is a noticeable additional decrease in signal at full strength. In contrast, later time points (PLD >1825 ms) show almost no difference in signal when gradients are applied.

2.3.2 Time-dependent behavior of signal

Figure 2.4 shows the behavior of the average normalized signal through time for the whole studied population. The first column corresponds to the arterial signal, and the second column the gray matter. The top row compares the signal with different crusher gradient strengths (eTE = 0 ms) and the bottom row shows variable echo times (without crushers). The shape of these curves differs from the typical "Buxton curve" [95] because of the variable lengths of the labeling blocks of the Hadamard encoding. The extent of crushing of the arterial signal can be appreciated in 2.4a, where the high signals for PLDs shorter than 1 second are almost completely removed by the application of even the lowest crusher strength.

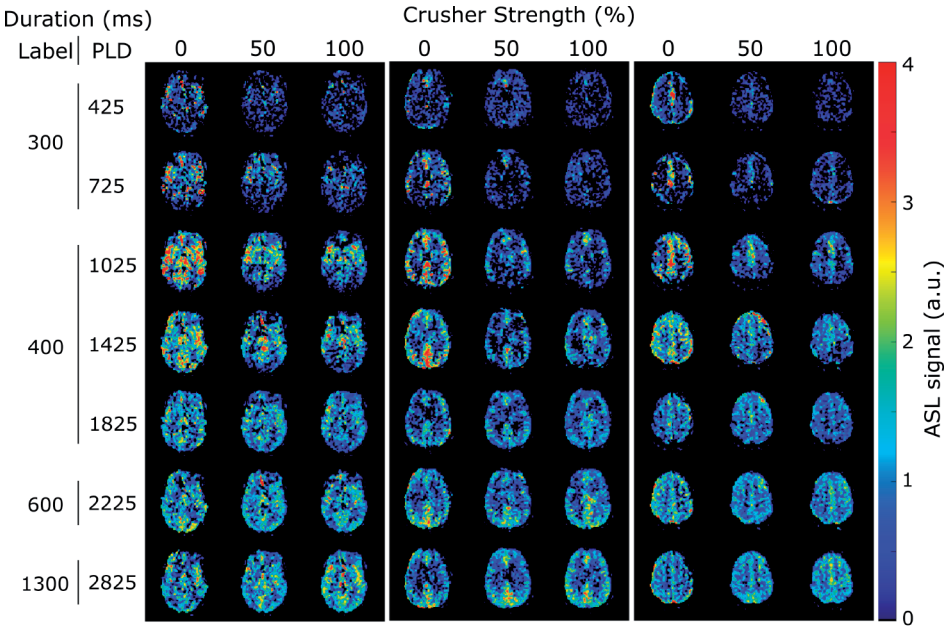

Figure 2.3. ASL signal maps with variable crushing at all time points in three slices of one subject. All images were acquired with an eTE of 0 ms. eTE: effective echo-time. PLD: post-labeling delay.

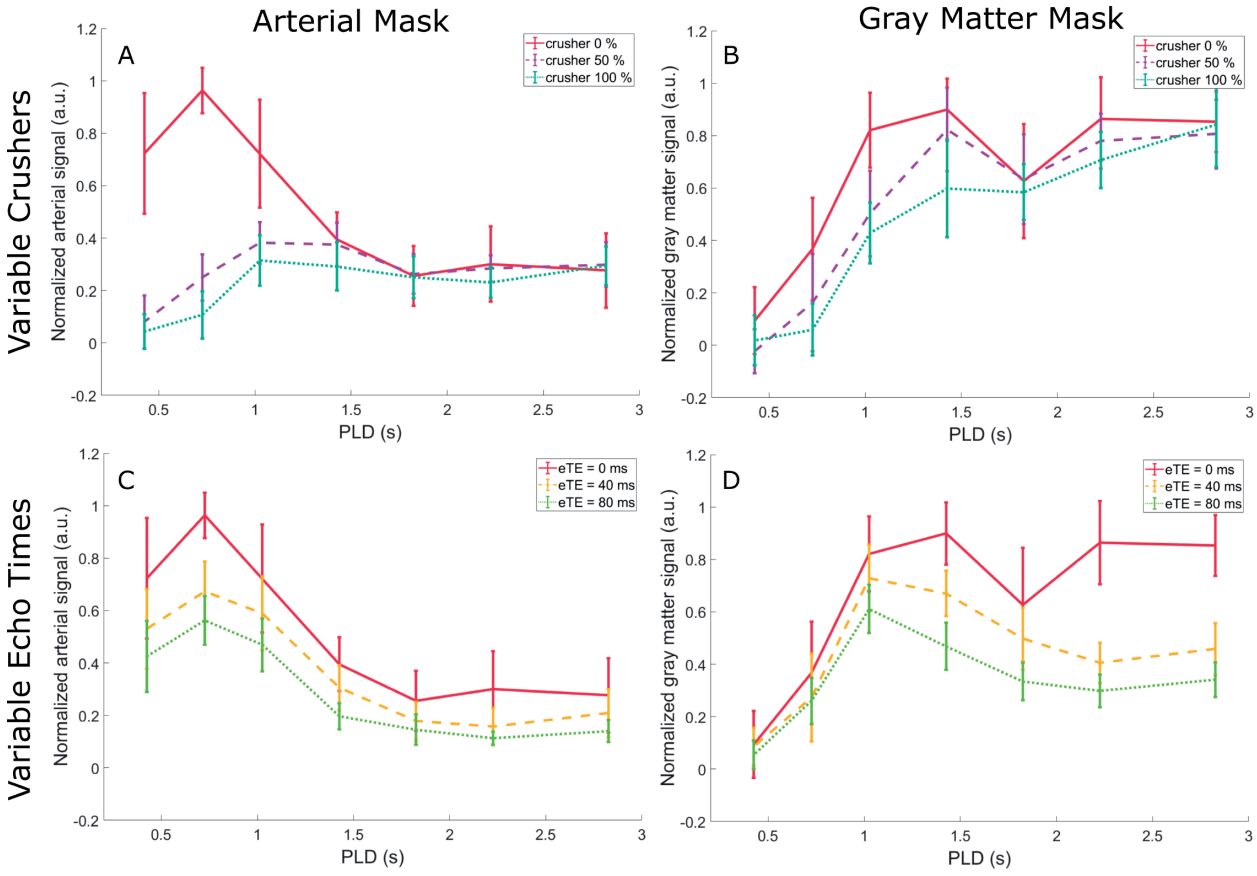

Figure 2.4. Average normalized gray matter and arterial signal through time, showing effects of crushers and echo times. Error bars indicate the SEM of the subjects. eTE: effective echo-time. PLD: post-labeling delay.

Doubling the gradient strength provides an additional reduction in signal. At later time points, there is almost no effect from the gradients. The graph in 2.4b reveals that the effect of gradients on the gray matter (perfusion) signal is lower than in arteries, but also most apparent for early PLD's. In Figure 2.4c and d, it is clear that with longer eTE's the signal is smaller (as expected) both for the vascular and tissue ROIs. This serves as a representation of the different mechanisms of the two methods: while the T_2-prep module affects the signal in all compartments (the signal is reduced at all time points, no matter where it is situated along the vascular tree or in the tissue), the gradients, by their nature, only remove the signal from flowing spins above a certain cutoff velocity, and the amount of label that is crushed and how deep into the vasculature depends on their b-value. This can be seen in the difference between the shapes of the gradient curves in a and b, which show that different gradient parameters lead to different timings for the arterial peak as well as shapes of the transition along PLD's.

2.3.4 Two-Compartment Dynamic Modeling

Figure 2.5 a-c shows the first step of the compartmental model fitting: the separation of the ASL signal into intravascular and extravascular components. The $T2_{EV}$ values from the fit of the unsubtracted images were 48±9 ms, 47±8 ms and 46±9 ms, for the weakest to strongest gradient. The $T2_{IV}$ was estimated to be 240 ms, 300 ms and 300 ms (highest permitted value) in the same order (the error on the fit of these values exceeds the values themselves). It can be observed that the intravascular signal (red dotted line) follows the expected time course: a high early peak followed by a subsequent decrease and an almost complete elimination of the signal. The extravascular component on the other hand displays more erratic behavior, although it tends to increase for longer PLDs.

The dynamic fit to the modified Buxton model (eq. 2.4) can be found in the bottom row (figure 2.5 d-f). The arterial transit time, δa, extracted from this fit was 620 (95% CI: 480-750) ms, 910 (720-1110) ms and 930 (690-1180) ms for gradients strengths of 0, 50, and 100%, respectively, and the tissue transit time δ_t, 2140 (1900-2390) ms, 1610 (1390-1830) ms and 2010 (1670-2350) ms, for a resulting BBB transition time Tex of 1520 ms, 700 ms and 1080 ms. These values are consistent with literature[102,111,112,153,154] (considering that they combine effects from all gray matter regions) and the uncrushed signal is associated with lower δ_a and narrower confidence intervals than the crushed. In contrast, the δ_t, exhibits a less clear relationship to the amount of crushing.

2.3.5 Comparison of Intravascular Fractions

In figure 2.6, the intravascular fractions as calculated with both techniques are compared. This refers to the IVF as described by the difference in signal between the crushed and uncrushed data, and $\Delta M_{IV} / (\Delta M_{IV} + \Delta M_{EV})$, that results from the fitting of equation 2.3 to the

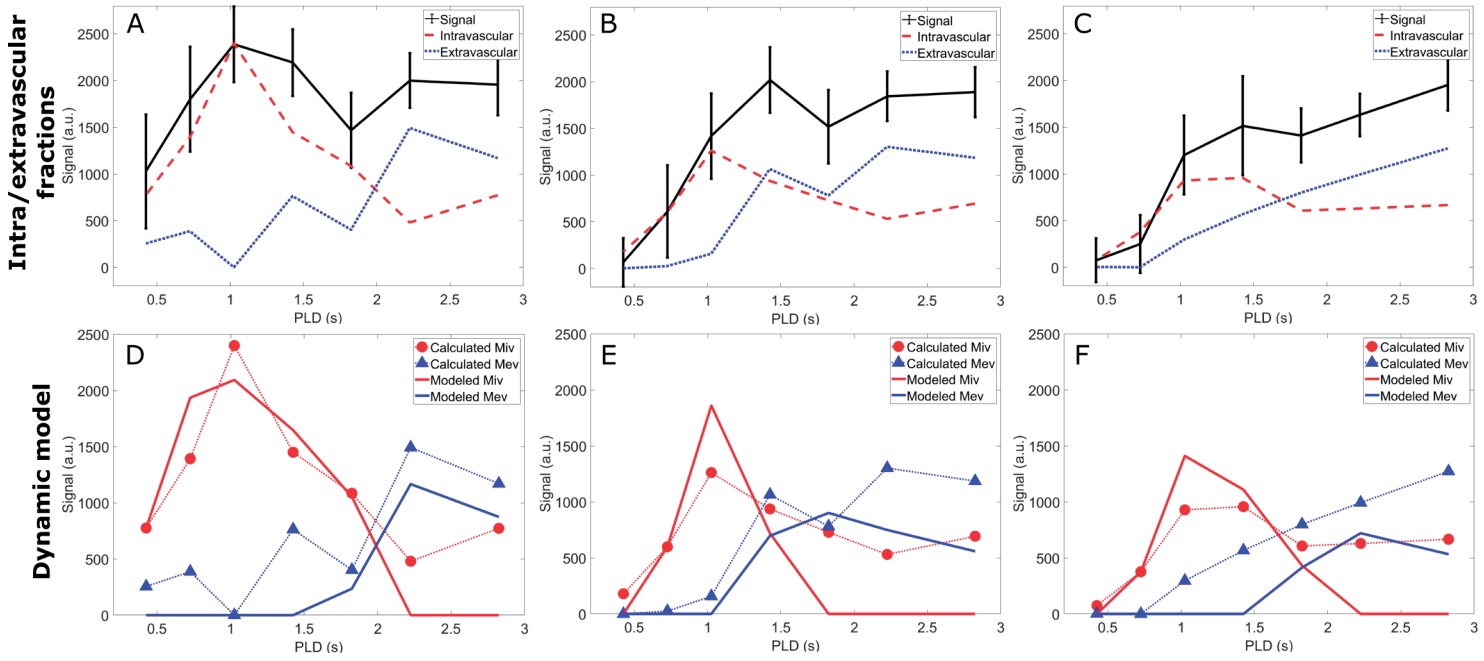

Figure 2.5. Results of the dynamic model fitting. In the top row, the ASL signal is broken down into intravascular and extravascular components (Δ_{MIV} and Δ_{MEV}, respectively) using T_2 differences (equation 2.3). On the bottom row, these same components (dotted lines with markers) are fitted to equation 2.4 and the resulting dynamic fit is given by the solid lines (red for intravascular, blue for extravascular). This analysis was performed on the population average data, and repeated for all three applied gradient strengths (no gradient in left column to highest gradient strength on the right). Confidence intervals were calculated for each point in the fit but were too large to be shown here.

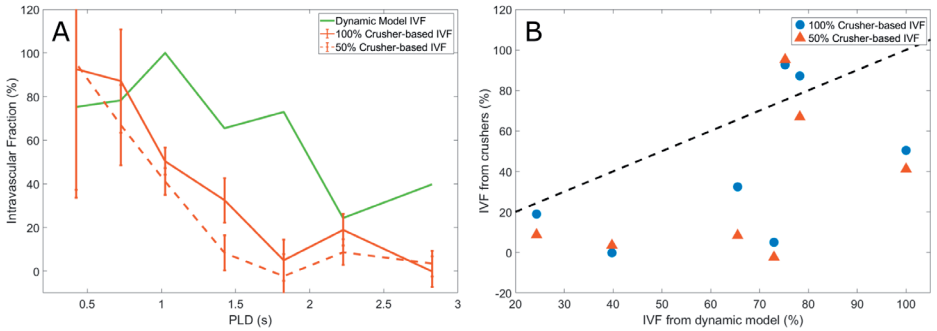

Figure 2.6. Comparison of the intravascular fractions as calculated with both methods. In A, the IVF's are shown through time, for the crusher gradient technique (orange) and the compartmental model applied to the variable eTE data (green). In B, a scatterplot shows the direct comparison of IVF values from both techniques (the black dotted line represents a perfect match).

TRUST data. The ΔM calculation is performed on the total signal with contributions from both the vasculature and the tissue, so, in this figure, the IVF is also calculated by combining the signal from the arterial and gray matter masks. In a, the time course of these fractions is shown. With both methods, the IVF observes a negative trend as the labeled water travels from the arteries into the tissue. However, the TRUST-based IVF is almost systematically higher than the crusher-based IVF. This is made clear in figure 2.6 b, where a scatterplot of the values for both methods is shown, highlighting the relative underestimation of the IVF in the gradients method. Furthermore, a paired Student's t-test (using the different PLD's as samples) was performed which showed a statistically significant difference between the TRUST-based IVF and the 50% gradient IVF ($p=0.037$) and a non-significant difference between the TRUST-based IVF and the 100% gradient ($p=0.090$), demonstrating that both gradient strengths underestimate the amount of intravascular signal, and substantially stronger gradients would be needed close the gap and lead to a measurement of IVF that is consistent with values estimated by the TRUST method.

2.3.6 Analysis of 3D dataset

Figure 2.7 shows the T_2-maps in gray matter as a function of PLD. The transition from high T_2-values, concentrated in the arteries for early PLDs, to lower T_2-values distributed across the gray matter for later PLDs is readily apparent. Differences between brain regions are also seen, particularly at PLD = 1825 ms, where a higher T_2 is present in the posterior brain region. Figure 2.8 shows the results of the dynamic analysis performed on a voxel-by-voxel basis, represented by maps of the arterial transit time δ_a (top row), the tissue transit time δ_t (middle row) and transit time across the BBB T_{ex} (or δ_t-δ_a, bottom row).

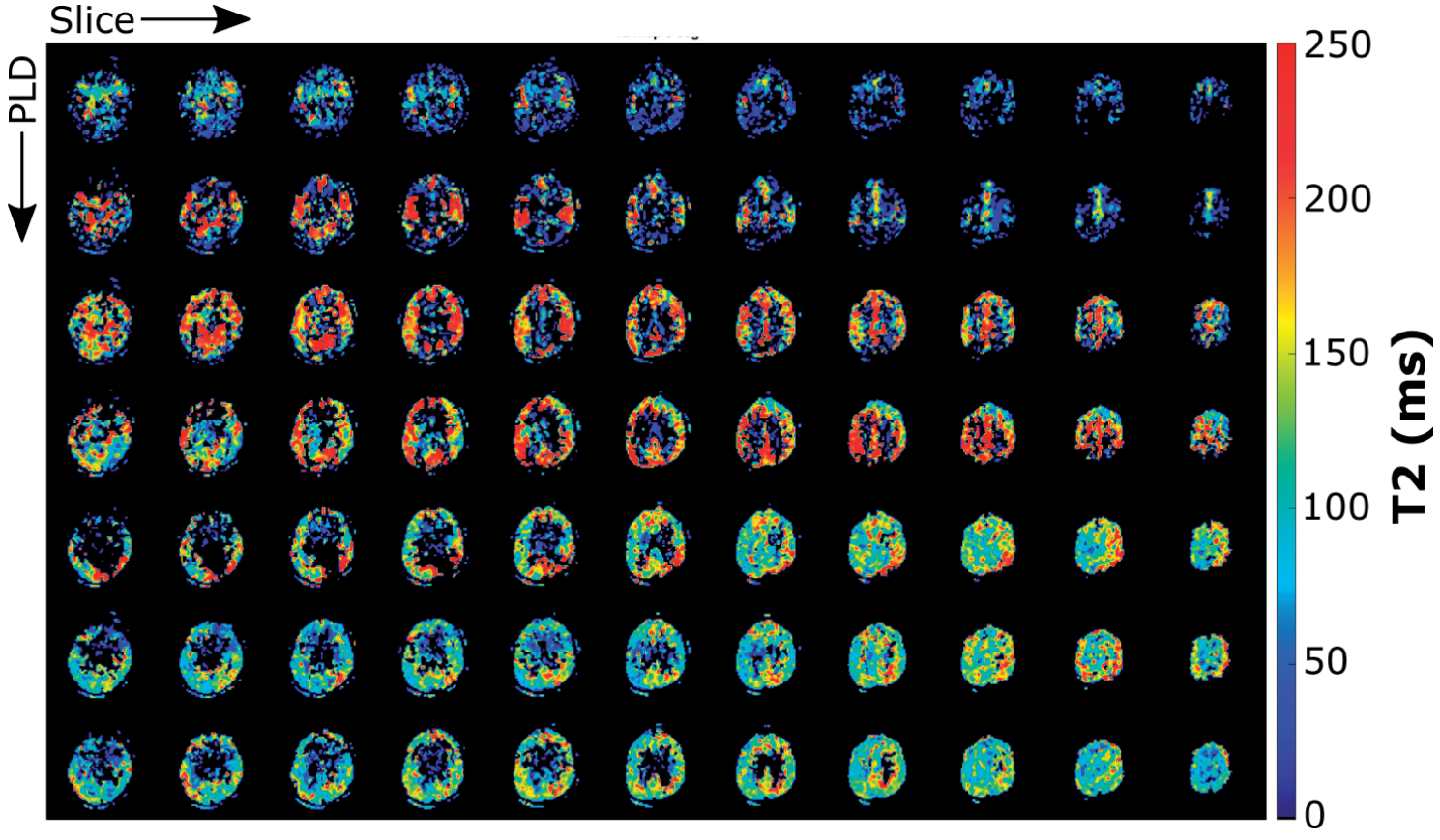

Figure 2.7. Map of the T2 calculated on the 3D-acquired dataset with the TRUST technique, for all time points.Voxels with an uncertainty on the fit higher than 200 ms or lower than 0.5 ms were removed from this image (ill-fitting points).

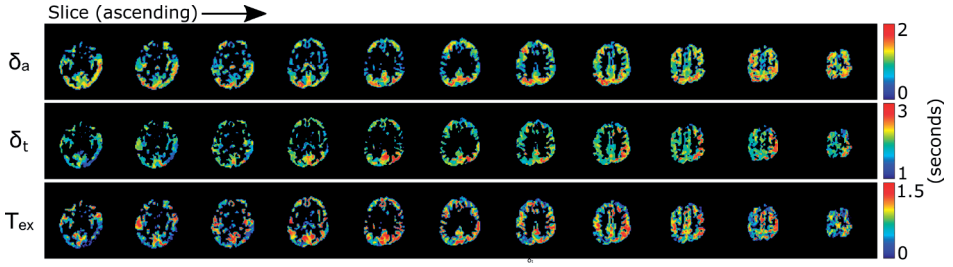

Figure 2.8. Results of the dynamic compartmental analysis on the 3D dataset performed on a voxel-by-voxel basis. Only the gray matter is shown, as the arteries are not suitable for this type of fit, and the white matter signal is too low for fitting.

2.4 DISCUSSION

In this study, the TRUST and crusher gradient methods were combined into a single ASL sequence to compare their properties when measuring water transport across the BBB. Measuring the two different approaches in a single sequence is important, since cerebral physiology is notoriously variable, e.g. depending on end-tidal CO_2 and alertness[155]. While both methods allow the separation of intravascular from extravascular signal to a certain extent, their mechanisms differ in key manners. The main findings of this study were threefold.

Firstly, the employed crusher gradients did not affect the entirety of the arterial signal. This is qualitatively apparent in the perfusion maps of figure 2.3. At the two shortest PLD's (425 and 725 ms), where arterial signal is prominent on the uncrushed images, there is still some signal left when crusher gradients are applied. This conclusion is also supported by figure 2.4a, where a qualitative look at the shape of the curves shows that the arterial peak is strongly attenuated by the application of gradients, but the initial increase and subsequent decrease in early time points for crushed signal curves indicates the presence of residual label in the arteries. The results shown in figure 2.5 also point to this conclusion. When the same fit, separating the intravascular from the extravascular signal based on their T_2 values, is performed on the crushed data, an arterial peak indicating the presence of intravascular signal is seen, even when using the strongest gradient. The longer δ_a values calculated with these data reflect the fact that the fastest flowing spins (those that arrive the earliest in the imaging plane) are removed by the gradients, resulting in a longer arrival time for the arterial spins that do make it to the imaging area. Moreover, the comparison between the intravascular fractions obtained with the two methods (figure 2.6b) shows a systematic underestimation of the fraction by gradients (statistically significant in the case of the weaker gradient), revealing their limited reach into the microvasculature and the difficulty in isolating the entirety of the blood pool signal. These IVF values are comparable to those obtained by St-Lawrence

et al.[131], who also looked at the fraction of signal located in the microvasculature at different PLD's with ASL. Their results for the intravascular fraction are on the same order of magnitude, but lower than both our TRUST and gradients methods results, likely because their technique, with its stronger gradients, allows the separation of the signal more specifically in the capillaries and not the whole of the vasculature.

The imperfect arterial signal cancellation resulting from the application of gradients can be explained by various factors. Firstly, gradients only work perfectly for flow which has a sufficient velocity component parallel to their orientation. Additionally, the crusher gradient method relies on a parabolic flow profile in the vessels[156] which may not be true in all vessels. At the capillary level, pseudo-random orientation of the capillaries can lead to signal saturation as is exploited in IVIM[157]. Because of the relatively low b-value (even when looking at our highest b-value) employed in the current study, this will only lead to an approximately 18% decrease in signal when assuming a D× of 0.02 mm^2/s[157]. Stronger gradients would allow crushing further into the vascular tree, but in our gradient echo sequence the concomitant increase in TE resulting from the need to create space for even stronger gradients, would result in too low SNR. Moreover, we note the inherent variability of the effect of gradients, which changes among others with the blood flow velocity (see for example the difference in IVF's between the two gradient strengths in figure 2.6), meaning that variations in blood velocity between subjects, or at different times, or caused by other factors, will result in differences in the fraction of the vasculature that is targeted.

Second, TRUST is a better tool to differentiate between the capillary and tissue compartments compared to the (relatively weak) gradients used in this study. In figures 2.3 and 2.4, we demonstrate that the T_2-prep module affects the signal at all PLD's and therefore reaches the entirety of the vascular tree and the tissue, as opposed to crushers, whose reach into the vascular tree is dependent on the gradient strength. Figure 2.6 shows that crushers systematically underestimate the intravascular component of the signal when compared to the TRUST method, which can more comprehensively target the vasculature, no matter what eTE's are used.

This discrepancy is explained by the different mechanism of TRUST. Since this approach is based on the T_2 of water, which changes as it travels across the BBB, it discriminates between intra- and extravascular signal due to the differences in T_2, i.e. the biexponential decay. Therefore, there is no limit as to how deep into the vascular tree the T_2-prep module will probe, while on the other hand the b-value of the gradient, chosen to separate the vascular from the tissue compartment, dictates the extent to which gradients affect vascular signal. While differences in parameters for the TRUST technique can also affect results (for example the accuracy and precision of measured T_2 values are influenced by the echo times used[145]), the

choice of b-value will determine how close to the exchange-site the label is crushed. By using smaller b-values, like in this study, this will be weighted more towards the arterial side than for higher b-values, which will be closer to the exchange site, i.e. capillary signal.

Our third conclusion is that combining these techniques does not add value in BBB assessment , although it was essential to compare the two approaches. This is especially made clear by the quantitative dynamic compartmental analysis that we performed. This analysis requires only the multiple eTE (TRUST) data to measure δ_a and δ_t, and by extension T_{ex}. Performing it on the data with different crusher-strength (figure 2.5) provided shorter δ_a values for the uncrushed data, which is expected as the gradients remove signal from the fastest flowing (shortest δ_a) spins. This does not reveal supplementary information about the nature of the BBB transition, but only on vascular transport. Moreover, the CI's on the fit of the crushed data were significantly larger, because this model expects intravascular signal. Using only the TRUST technique is therefore sufficient to provide all the relevant information, and allows a shorter readout TE, boosting the overall SNR. This was demonstrated in an additional experiment that could now be done with a 3D readout. The 3D experiment did show that the TRUST technique can provide the desired results within a shorter sequence duration (18 min as compared to 50 min for the combined sequence), while also resulting in image quality high enough to allow whole brain voxel-wise T_2 mapping (figure 2.7) and arrival time mapping (figure 2.8 The δ_a map shows a pattern that is consistent with literature,[113,158] with the central part of the MCA flow territories showing shorter arrival times, just as in lower slices, whereas the posterior region exhibits longer arrival times. The δ_t map shows a less clear spatial dependence, although higher values seem to be present for areas with higher δ_a. Finally, the T_{ex} map, which is in fact the subtraction of the first two, by its nature highlights variations and noise that are present in the other maps. It is still possible to see that the pattern seems not to depend strongly on vascular territories, as for example high values are present in all parts of the brain. It appears that deeper cortical regions may be associated with longer T_{ex}, however a study including a larger sample of participants would be necessary to confirm this.

The main limitations affecting this study were the low signal-to-noise ratio (SNR) of our data as well as the limited strength of the gradients used. ASL is famously associated with low SNR as it is a subtractive technique, representing a few percent at most of the total signal in the brain. In this protocol, additional sequence modules reduced signal further, resulting in noisier data. As a consequence, a considerable amount of averaging was required. Not only was the signal averaged over the whole gray matter or arterial mask, it necessitated averaging over the studied population. This averaging was beneficial to counter the low SNR, however it lead to the inclusion of different flow territories, associated with variable arrival times[158], which in turn may have influenced the results of fitting. The main sequence

also took a long time to perform (~50 min) and an additional dataset with only one of these techniques showed that better SNR can be achieved in a shorter time frame when focusing on a single approach. Moreover, without the crusher gradients a shorter echo-time of the readout sequence could be employed, also resulting in a higher SNR. Additionally, our protocol focused on lower b-values and lacked a higher b-value which would allow a two-stage approach such as suggested by St. Lawrence et al[131] for a more quantitative measurement of water transport parameters. In its current form, our protocol cannot properly assess the actual transition across the BBB with the gradients method, as the gradient V_{enc} is not low enough to target blood flow in capillaries. Our choice for these strengths was made because the combination of T_2-prep and motion sensitizing gradients was more easily done with a gradient echo readout as compared to spin echo. Longer gradients would have led, however, to too much signal loss due to T2* and thus to further lowering the SNR, which was already an issue with our protocol. Moreover, a limitation of the TRUST method as applied in this study should be mentioned. To stabilize the dynamic model fit, we applied in equation 2.3 the assumption that the intravascular T_{2iv} is constant for all PLDs. This assumption is based on the rapid exchange of water with tissue when the capillary bed is reached. While changes in oxygenation occur along the whole length of the microvasculature, which takes 2s or more on average[159], extravasation of water is more rapid (0.2-1s)[129,131,160], which means most of the water moves to the tissue before significant changes in oxygenation occur. Because the T_2 of blood is strongly dependent on oxygenation[146], further into the capillary bed our assumptions will fail. The uncertainty on the calculated T_{2iv} was high, which may be a result of the high variability of arterial signal for the early PLD's, combined with the notorious instability of bi-exponential fitting. Finally, while it is possible to add the gradients into the T_2-prep module, we decided against it for two reasons: first, with the varying duration and number of pulses of the T_2-prep, it is challenging to keep the crushing effects of the gradients similar (i.e. also for higher order moments). Second, as the crushing effects could not be guaranteed to be the same for all eTE's, an interdependency between the TRUST and gradient approach would be introduced, which would make it difficult if not impossible to separate these effects convincingly.

A limitation of our analysis protocol was the use of thresholding of perfusion images for gray matter and arterial masking. The resulting masks have been prone to some contamination, in particular some of the arterial signal could still be included in the gray matter. Using a T_1-weighted image would have allowed a standard delineation of brain regions, however, at the low resolution used for ASL, there will always be partial voluming issues, and it is not possible to remove all contamination from arteries and white matter. Thresholding was therefore deemed sufficient for this analysis.

In conclusion, our comparison of the use of crusher gradients and TRUST to measure the transport of water across the BBB showed that TRUST provides a more accurate and complete picture of this process than crusher gradients, because TRUST can separate the signal from spins in the vasculature and those in tissue, while with gradients only part of the intravascular signal is effectively excluded. Moreover, it has been shown that a full TRUST protocol can be performed in a reasonable scan time and with high enough SNR to provide voxel-wise and regional BBB assessments . It would remain to be studied whether the use of much stronger crusher gradients might alleviate some of these issues.

2.5 ACKNOWLEDGEMENTS

This work is part of the research programme Innovational Research Incentives Scheme Vici with project number 016.160.351, which is financed by the Netherlands Organisation for Scientific Research.